INTRANODAL DEPLETION EFFECTS IN MOX CORES

Petri Forslund and Erwin Müller
ABB Atom AB
SE-72163 Västerås, Sweden
petri.forslund@se.abb.com ; erwin.muller@se.abb.com

Sten-Örjan Lindahl
Studsvik Scandpower AB
SE-72212 Västerås, Sweden
sol@quicknet.se

ABSTRACT

The modeling of depletion-history-induced intranodal effects on important neutron physical parameters in nodal diffusion theory is addressed. Consideration is given to a situation where these aspects are of particular importance, namely, in mixed oxide cores where strong interaction between uranium and plutonium mixed oxide assemblies occur. Numerical studies on selected models are performed in order to evaluate their relative merits. It is demonstrated that intranodal effects have to be accounted for in order to obtain accurate pin power predictions. It is also found that the combined use of intranodal isotopic inventory and exposure distributions for estimating intranodal cross section behaviour significantly improves the accuracy in pin powers over the more traditional approach of utilizing exposure distributions only.

1 INTRODUCTION

Modern nodal methods[1] are firmly established as standard design tools for Light Water Reactor (LWR) cores. Major contributors to the successful application of these methods have been the introduction of advanced homogenization and dehomogenization methods[2–4] as well as the early development of various nodal models and intranodal flux reconstruction techniques. Recently, considerable efforts in the further development of nodal cross section models and in particular of the treatment of depletion history effects and intranodal cross section behaviour have been made. This has led, inter alia, to the introduction of microscopic depletion models,[5–11] intranodal cross section models,[12] and a variety of spectral interaction and spatial rehomogenization techniques.[13–16] All of these methods attempt to compensate, at the level of the global nodal solution, for the deficiencies inherent in the standard nodal cross section generation procedure based

on single-assembly (SA) lattice depletion calculations*. Alternatives, such as employing multi-assembly lattice depletion calculations or generating nodal parameters as a function of surface leakages[2,17,18] are usually considered impractical due to the large number of lattice calculations necessary for such approaches to be succesful or due to the large volume of tabulated data which accompanies such approaches.

Those methods which utilize nodal calculational results directly in order to correct the cross sections for deficiencies inherent in the preselected boundary conditions and depletion histories employed during the single-assembly depletion calculations, are considered most attractive because of their efficiency and practicality. However, there is some concern as to the basic assumptions and hence the accuracy of some of the models employed in this type of approach. One such aspect which deserves detailed analysis is the impact of depletion-history-induced intranodal effects on the nodal solution and reconstructed heterogeneous parameters (e.g., pin powers). The main challenge in this regard, is to find a practical method to determine an accurate spatial representation for the intranodal cross sections. In this paper two possible approaches for solving this problem are investigated, namely, by utilizing explicit exposure values at selected intranodal locations or the combination of both exposure and isotopic number density values at these same locations in order to determine the intranodal cross section shape. In both instances the cross section spatial dependence is represented by a second or fourth order Legendre polynomial.

Modeling depletion-history-induced effects are of particular importance when strong neutronic interaction occurs between fuel assemblies, such as encountered in Pressurized Water Reactor (PWR) mixed MOX/UO_2 cores. In order to provide a simplified analysis of intranodal cross section shapes, an one-dimensional two-group diffusion theory problem representing a typical PWR MOX/UO_2 configuration sufficiently severe to challenge the proposed models was considered in this study. Complications resulting from various approximations necessary for solving multi-dimensional problems are thereby eliminated since a rigorous analytic solution can be found for the one-dimensional diffusion equation. For physical reasons, at least two energy groups must be considered to realisticaly account for neutronic interaction between material regions (e.g., MOX/UO_2).

In section 2 the theory of the intranodal cross section model is presented. In addition, the analytical solution to the diffusion equation and the formalism used for pin† power reconstruction are described. The PWR MOX/UO_2 slab benchmark problem used in this work is defined in section 3 and the numerical analysis is presented in section 4. Finally, section 5 provides concluding remarks.

2 THEORY

A basic requirement for the successful application of modern nodal methods is that accurate equivalent nodal parameters (cross sections, discontinuity factors, form functions) are available. While theoretically rigorous homogenization techniques have been developed for time-independent problems, these methods do not provide unambiguous prescriptions for treating depletion-induced effects. This problem is partly solved by tabulating equivalent nodal parameters as a function of predefined depletion history conditions. However, additional adjustments of the nodal cross sections are necessary in order to account for the deviations of the true depletion history from these predefined idealized conditions. In this regard, the usual approach is to impose some intranodal spatial dependence on the nodal cross sections. Consequently, the solution of the

*In these single-assembly calculations, idealized boundary conditions (e.g., reflective) and selected depletion history conditions, which in general may not be representative of the real core situation, are normally applied.

†The notion of a pin is used here even if it is actually a slab in one dimension.

diffusion equation with spatially dependent coefficients and the determination of the intranodal cross section behaviour have to be considered. In the following, the approach used in this work to address these two issues is presented. The closely related topic of pin power reconstruction is also discussed.

2.1 SOLUTION OF THE DIFFUSION EQUATION

Consider the one-dimensional G-group diffusion equation

$$\frac{\mathrm{d}}{\mathrm{d}x}\hat{D}(x)\frac{\mathrm{d}\vec{\phi}(x)}{\mathrm{d}x}+\hat{\Sigma}(x)\vec{\phi}(x)=\vec{0} \tag{1}$$

where $\vec{\phi}(x)$ is the Gx1 flux vector, $\hat{D}(x)$ is the GxG diagonal matrix of diffusion coefficients and $\hat{\Sigma}(x)$ is the GxG cross section matrix. The diffusion coefficients are assumed to be nodewise constant while the cross sections are taken to be smoothly varying within each node. For node n this cross section dependence is given by

$$\hat{\Sigma}_n(\xi)=\hat{\Sigma}_n^{\mathrm{ave}}+\Delta\hat{\Sigma}_n(\xi) \tag{2}$$

where $\hat{\Sigma}_n^{\mathrm{ave}}$ is the node average cross section and ξ is the local dimensionless coordinate

$$\xi=(2/h_n)x;\ -(h_n/2)\leq x\leq(h_n/2)$$

for the node of size h_n.

The nodal approach of solving the diffusion equation consists of two steps. Firstly, a neutron balance equation is derived by integrating eq. (1) over the volume of a given node n with neighbours m,

$$\frac{1}{h_n}\sum_{m=1}^{2}\vec{J}_{mn}-\left(\hat{\Sigma}_n^{\mathrm{ave}}+\Delta\hat{\Sigma}_n^{\mathrm{spatial}}\right)\vec{\phi}_n=\vec{0} \tag{3}$$

where $\Delta\hat{\Sigma}_n^{\mathrm{spatial}}$ is defined energy groupwise as

$$\Delta\Sigma_{ngg'}^{\mathrm{spatial}}=\frac{\int_{-1}^{+1}\Delta\Sigma_{ngg'}(\xi)\phi_{ng'}(\xi)\mathrm{d}\xi}{\int_{-1}^{+1}\phi_{ng'}(\xi)\mathrm{d}\xi} \tag{4}$$

Secondly, a relationship between surface-averaged outward-directed (from node n) net currents $\vec{J}_{mn}$ and the node-averaged fluxes of neighbouring nodes n and m is found in the form of

$$\vec{J}_{mn}=\hat{C}_{mn}\vec{\phi}_n-\hat{C}_{nm}\vec{\phi}_m \tag{5}$$

By using these two equations a coupled set of non-linear equations for the global problem is obtained with node-average fluxes as unknowns which is solved by means of standard numerical iteration techniques.

Nodal methods differ mainly in the manner in which the so-called coupling coefficient matrices $\hat{C}_{mn}$ are determined. In the analytic approach an analytic solution[19,20] to the diffusion equation within a given node

is used for this purpose. To obtain this solution, eq. (1) is rewritten* in the following form (dropping index n)

$$\frac{4}{h^2}\hat{D}\frac{\mathrm{d}^2\vec{\phi}(\xi)}{\mathrm{d}\xi^2} + \left(\hat{\Sigma}^{\mathrm{ave}} + \Delta\hat{\Sigma}^{\mathrm{spatial}}\right)\vec{\phi}(\xi) = \underbrace{\left(\Delta\hat{\Sigma}^{\mathrm{spatial}} - \Delta\hat{\Sigma}(\xi)\right)\vec{\phi}(\xi)}_{\vec{S}(\xi)} \tag{6}$$

Assuming a polynomial form for the right-hand-side,

$$\vec{S}(\xi) \equiv \left(\Delta\hat{\Sigma}^{\mathrm{spatial}} - \Delta\hat{\Sigma}(\xi)\right)\vec{\phi}(\xi) \approx \sum_{l=1}^{L}\vec{s}_l P_l(\xi) \tag{7}$$

the general solution is given by

$$\begin{aligned}\vec{\phi}(\xi) \;=\; & \cos(\sqrt{\hat{B}^2}\,\xi)\,[\cos(\sqrt{\hat{B}^2})]^{-1}\left(\tfrac{1}{2}(\vec{\phi}_+ + \vec{\phi}_-) - \textstyle\sum_{l_{\mathrm{even}}}\vec{d}_l\right) \\ & + \sin(\sqrt{\hat{B}^2}\,\xi)\,[\sin(\sqrt{\hat{B}^2})]^{-1}\left(\tfrac{1}{2}(\vec{\phi}_+ - \vec{\phi}_-) - \textstyle\sum_{l_{\mathrm{odd}}}\vec{d}_l\right) \\ & + \textstyle\sum_{l=0}^{L}\vec{d}_l P_l(\xi)\end{aligned} \tag{8}$$

where $\vec{\phi}_\pm$ are the left (-) and right (+) node side fluxes and the coefficients $\vec{d}_l$ are functions of $\hat{B}^2$, $\hat{D}$ and $\vec{s}_l$. In the above $P_l(\xi)$ represents the Legendre polynomial of order l and

$$\hat{B}^2 = \frac{h^2}{4}\hat{D}^{-1}\left(\hat{\Sigma}^{\mathrm{ave}} + \Delta\hat{\Sigma}^{\mathrm{spatial}}\right) \tag{9}$$

In order to determine the spatial cross section correction $\Delta\hat{\Sigma}^{\mathrm{spatial}}$ defined in eq. (4), a Legendre polynomial expansion is used individually for the intranodal flux and for the cross section distributions whereas the source polynomial expansion coefficients $\vec{s}_l$ are computed by fitting a Legendre polynomial directly to discrete values of the intranodal source $\vec{S}(\xi)$ given by eq. (7).[12]

2.2 CROSS SECTION MODEL

The node average cross section $\hat{\Sigma}^{\mathrm{ave}}$ is estimated as

$$\hat{\Sigma}^{\mathrm{ave}} = \hat{\Sigma}^{\mathrm{SA}}(E) + \sum_{i=1}^{I}\hat{\sigma}_i^{\mathrm{SA}}(E)\left(N_i(E) - N_i^{\mathrm{base}}(E)\right) \tag{10}$$

where $\hat{\Sigma}^{\mathrm{SA}}$ and $\hat{\sigma}^{\mathrm{SA}}$ are single-assembly macroscopic and microscopic cross sections tabulated as a function of the node average exposure E. The last term in this expression represents a correction to the single-assembly macroscopic cross sections for number density changes relative to the nuclide inventory obtained during single-assembly depletion calculations.[5,6,11] The base number density $N_i^{\mathrm{base}}(E)$ is obtained by performing nodal depletion calculations at the same physical conditions as applied during the single-assembly

*Theoretically, the $\Delta\hat{\Sigma}^{\mathrm{spatial}}$ terms on both sides of eq. (6) could be eliminated, but for consistency the node average cross section appearing in the balance eq. (3) is used on the left-hand-side of eq. (6).

depletion calculations. The number density $N_i(E)$ is obtained from nodal depletion calculations at the real conditions. It should be noted that the calculation of both types of number densities must be synchronized with regard to depletion step sizes in order to avoid inconsistencies. This approach differs from some other so-called microscopic depletion models[7–10] in which $N_i^{\text{base}}(E)$ is taken to correspond exactly with base number densities computed by the lattice code.

The intranodal cross section variation $\Delta\hat{\Sigma}(\xi)$ around the average cross section is defined such that its integral over node volume is zero. A functional representation of $\hat{\Sigma}(\xi)$ is required to facilitate the analytic solution of the diffusion equation. If discrete values of this cross section distribution were available, then a polynomial fit of finite order could be generated as

$$\hat{\Sigma}(\xi) = \hat{\Sigma}^{\text{ave}} + \sum_{l=1}^{L} \hat{a}_l P_l(\xi) \tag{11}$$

The problem is to determine the required discrete values of the intranodal cross section. In this work two approaches to resolve this problem are considered.

In the first approach discrete exposure values are used to interpolate in the single-assembly cross section tables to compute

$$\Delta\hat{\Sigma}(\xi_k) = \hat{\Sigma}^{\text{SA}}(E_k) - \hat{\Sigma}^{\text{SA}}(E) \tag{12}$$

where E_k is the exposure at the location ξ_k and E is the node average exposure. This model is referred to as **sidbur-2nd** for a second order ($L = 2$) and **sidbur-4th** for a fourth order ($L = 4$) spatial representation.

In the second approach both exposures and isotopic inventories are utilized to compute

$$\begin{aligned} \Delta\hat{\Sigma}(\xi_k) \quad = \quad & \hat{\Sigma}^{\text{SA}}(E_k) - \hat{\Sigma}^{\text{SA}}(E) \\ & + \textstyle\sum_{i=1}^{I} \left[\hat{\sigma}_i^{\text{SA}}(E_k)\Delta N_i^k - \hat{\sigma}_i^{\text{SA}}(E)\Delta N_i\right] \end{aligned} \tag{13}$$

where

$$\begin{cases} \Delta N_i^k = N_i(E_k) - N_i^{\text{base}}(E_k) \\ \Delta N_i = N_i(E) - N_i^{\text{base}}(E) \end{cases} \tag{14}$$

This model is referred to as **sidmic-2nd** for a second order ($L = 2$) and **sidmic-4th** for a fourth order ($L = 4$) spatial representation. In addition, the model option **nointra** ignoring intranodal dependencies by using node-averaged quantities only is considered for the purpose of comparison.

2.3 PIN POWER RECONSTRUCTION

A modulation approach is applied for reconstructing detailed heterogeneous pin powers

$$P^{\text{het}}(\xi) = p^{\text{SA}}(\xi) \sum_{g=1}^{G} \kappa\Sigma_{fg}(\xi)\phi_g(\xi) \tag{15}$$

where $p^{SA}(\xi)$ is the single-assembly power form function. In the above, the analytical flux solution given by eq. (8) is used in combination with an intranodal kappa-fission cross section ($\kappa\Sigma_f$) defined according to eq. (11).

In practice, integration of eq. (15) over each pin domain is approximated by separately integrating each of the factors appearing in the expression.

3 DEFINITION OF THE PWR MOX/UO_2 TEST PROBLEM

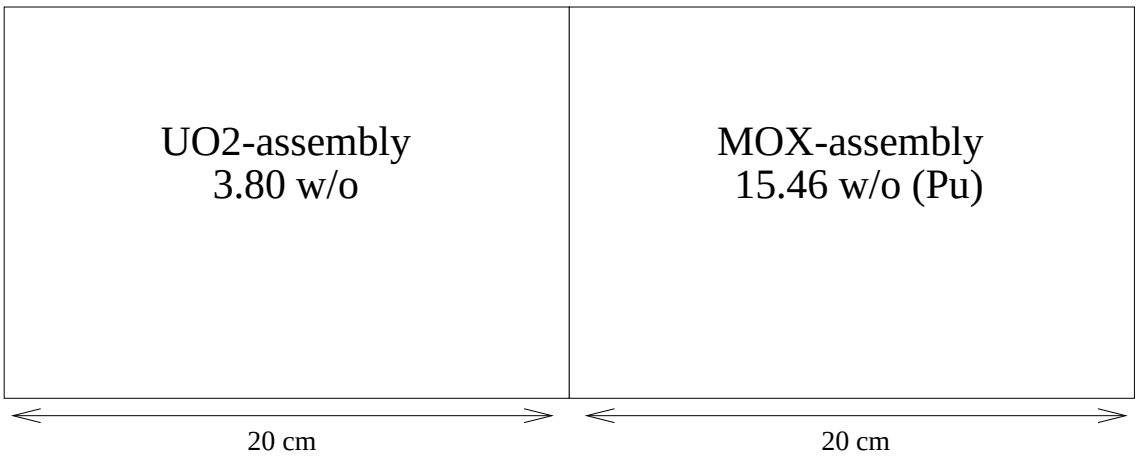

Figure 1. Schematical illustration of the PWR MOX/UO_2 benchmark with periodic boundary conditions.

In figure 1 the material layout and dimensions of the one-dimensional PWR MOX/UO_2 problem used in this work are shown. The problem consists of a homogeneous UO_2 slab and a homogeneous MOX slab loaded in a checkerboard manner. The homogeneous nature of this configuration allows a direct comparison of homogeneous intranodal distributions (e.g., pin-integrated powers, burnups, cross sections, fluxes) with the corresponding homogeneous reference distributions generated via pointwise depletion. This is due to the fact that for homogeneous assemblies all form functions and discontinuity factors are flat and unity.

Two-group, spatially smeared, microscopic and macroscopic cross sections, representative of realistic 17x17 PWR-fuel configurations were utilized. The average enrichment of the UO_2-assembly is 3.80 w/o whereas the Pu content of the MOX assembly is 15.46 w/o. Neither assembly type contains burnable absorbers. Both the whole core reference and the single-assembly depletion calculations were performed on a fine spatial mesh (0.5 cm). The same mesh size was used to represent the pin regions. The subsequent nodal calculations utilized assembly mesh sizes (20 cm) in conjunction with the exposure-dependent cross sections produced by the above single-assembly calculations *. A typical PWR power density of 37 W/g was used in the depletion calculations.

*The single-assembly power form function has a constant value of unity in this problem ($p^{SA}(\xi) \equiv 1.0$) and does not contribute to the heterogeneous pin power.

4 NUMERICAL RESULTS

The methods described in section 2 have been implemented in a computer code. All calculations, including the reference and single-assembly calculations mentioned in section 3, were performed with this code. The discretized diffusion equation is solved by standard iterative techniques to obtain the multiplication factor (k_{eff}) and flux distributions. In all calculations a convergence criterion of 10^{-6} has been used for k_{eff} and nodal powers.

The models proposed in section 2 are compared againts the relevant whole core **reference** solution. The parameters which are compared are k_{eff}, nodal powers and pin powers. In addition, edits of pin-integrated exposures, fluxes and cross sections are also performed for comparison purposes. For the exposure distributions, Legendre polynomial expansions of the same order as used for the intranodal cross sections are utilized. Nodal powers and pin powers are normalized to the core volumetric power density and their errors are computed as differences multiplied with 100 (in units of per cent). k_{eff} errors are reported in units of pcm*. Errors in all other pin (index i) quantites are computed as

$$\begin{cases} \varepsilon_i = \frac{X_i - X_i^{\text{reference}}}{\overline{X}} \cdot 100\ \% \\ \Delta P_{\text{pin}}^{\text{MAX}} = \max_i |\varepsilon_i| \\ \Delta P_{\text{pin}}^{\text{RMS}} = \sqrt{\frac{1}{N_{\text{pin}}} \sum_i^{N_{\text{pin}}} \varepsilon_i^2} \end{cases}$$

where $\overline{X}$ is the node average value of the relevant parameter.

Table I. Summary of results for the MOX/UO_2 benchmark at 10 MWd/kg.

Calculation Method	k_{eff} Δk_{eff} [pcm]	P_{node} ΔP_{node} [%]		$\Delta P_{\text{pin}}^{\text{RMS}}$ [%]		$\Delta P_{\text{pin}}^{\text{MAX}}$ [%]	
		UO_2	MOX	UO_2	MOX	UO_2	MOX
Reference	1.30598	0.974	1.026				
Nointra	1.30689	0.974	1.026				
	91	0.0	0.0	2.3	3.0	6.0	11.7
Sidbur-2nd	1.30571	0.974	1.026				
	-27	-0.0	0.0	0.9	1.7	3.0	7.0
Sidbur-4th	1.30632	0.974	1.026				
	34	-0.0	0.0	1.2	1.8	3.3	7.0
Sidmic-2nd	1.30382	0.978	1.022				
	-216	0.3	-0.3	1.9	1.0	2.8	2.4
Sidmic-4th	1.30556	0.977	1.023				
	-42	0.2	-0.2	0.5	0.4	0.8	0.9

In table I, representative results for the different model options previously discussed are shown at a core depletion of 10 MWd/kg (approximately one cycle length). In all calculations utilizing fourth order expansions ($L = 4$) the required additional intranodal points have been selected to be 2.0 cm from the node boundaries. This choice is based on auxiliary numerical studies in which the impact on the pin powers of different intranodal positions were evaluated using the model option **sidmic-4th**. The results from these studies show that any value between 2.0 and 4.0 cm would be adequate (approximately one epithermal mean free path).

*10^{-5} = 1 pour cent mille.

It is observed from the results in table I that global parameters, such as k_{eff} and nodal powers, are rather well predicted and less sensitive to the different intranodal models than the local parameters (pin powers). Furthermore, it is recognized that intranodal effects must be modeled in order to obtain accurate pin power predictions. Rather poor pin power prediction capability is obtained by utilizing only intranodal exposure distributions (**nointra**, **sidbur-2nd** and **sidbur-4th**) whereas the combined use of exposure and intranodal nuclide inventory distributions for determining the intranodal cross section behaviour (**sidmic-2nd** and **sidmic-4th**) clearly improves the pin powers, especially with regard to the maximum pin power error. The **sidmic-4th** is apparently the best method and yields pin power errors of less than 1 %.

It is often suggested[21] that pin power errors are mainly caused by deficiencies in the intranodal representation of $\kappa\Sigma_{fg}(\xi)$ in eq. (15), and not by the intranodal flux $\phi_g(\xi)$. This may be true for fresh cores but is not necessarily the case for depleted cores. In order to gain clarity in this matter a deeper analysis of the intranodal distributions is performed in the following.

In figure 2, the relative pin powers and the corresponding pin power errors of the different cross section models are shown whereas in figures 3 and 4 the relative errors in the pin-integrated kappa-fission cross sections and fluxes are presented.

From figure 2 it is seen that the cross section models using exposure distributions only (**nointra**, **sidbur-2nd** and **sidbur-4th**) have relatively large pin power errors at the node boundaries whereas in the interior of the node smaller errors are obtained. By studying the intranodal flux and cross section behaviour in more detail, as given by figures 3 and 4, it is observed that within the node the flux error approximately cancels the cross section error (especially in the thermal group) whereas near material boundaries no such cancellation effects are seen. However, it is important to bear in mind that all errors obtained for the flux are a pure consequence of the induced errors in the intranodal cross sections. This is due to the fact that an analytic approach of solving the one-dimensional diffusion equation has been employed here, as discussed in section 2.

The models utilizing the combination of exposure and nuclide inventory distributions (**sidmic-2nd** and **sidmic-4th**) incur an oscillating pin power error behaviour which is especially large for the **sidmic-2nd** model. Clearly a low order polynomial expansion does not fully capture the exponential character of the intranodal cross section and flux distributions near material boundaries. However, the **sidmic-4th** model represents an acceptable approximation to this exponential behaviour and yields pin power errors of less than 1 %. It is also noted that in the MOX assembly the thermal flux error counteracts the thermal kappa-fission error whereas in the epithermal group the opposite effect is seen. This has certain consequences because even if the epithermal kappa-fission cross section is small in magnitude compared to the thermal one ($\kappa\Sigma_{f1} \approx 1/30\ \kappa\Sigma_{f2}$), its error contributes significantly (i.e., to the same extent as the thermal group) to the observed pin power error in the MOX assembly due to the very hard spectrum there ($\phi_1 \approx 38\ \phi_2 \Rightarrow \kappa\Sigma_{f1}\phi_1 \approx 4/3\ \kappa\Sigma_{f2}\phi_2$). It is therefore the epithermal kappa-fission cross section error which dominates the obtained pin power error in the MOX assembly. On the other hand, in the UO_2 assembly the epithermal and thermal flux error distributions are similar to the corresponding kappa fission cross section error behaviour. As a consequence, no error cancellation effect occurs and a pin power error distribution similar to the kappa-fission cross section error is obtained. In the UO_2 assembly the thermal group is still more important than the epithermal group ($\kappa\Sigma_{f1}\phi_1 \approx 1/4\ \kappa\Sigma_{f2}\phi_2$) and gives the most significant contribution to the pin power error behaviour.

The above observations clearly demonstrate that it is not only the intranodal shape of the kappa-fission cross section which is important for pin power reconstruction. The intranodal representation of all the cross sections appearing in the diffusion equation have an equal importance for accurate pin power reconstruction via their impact on the intranodal flux distribution.

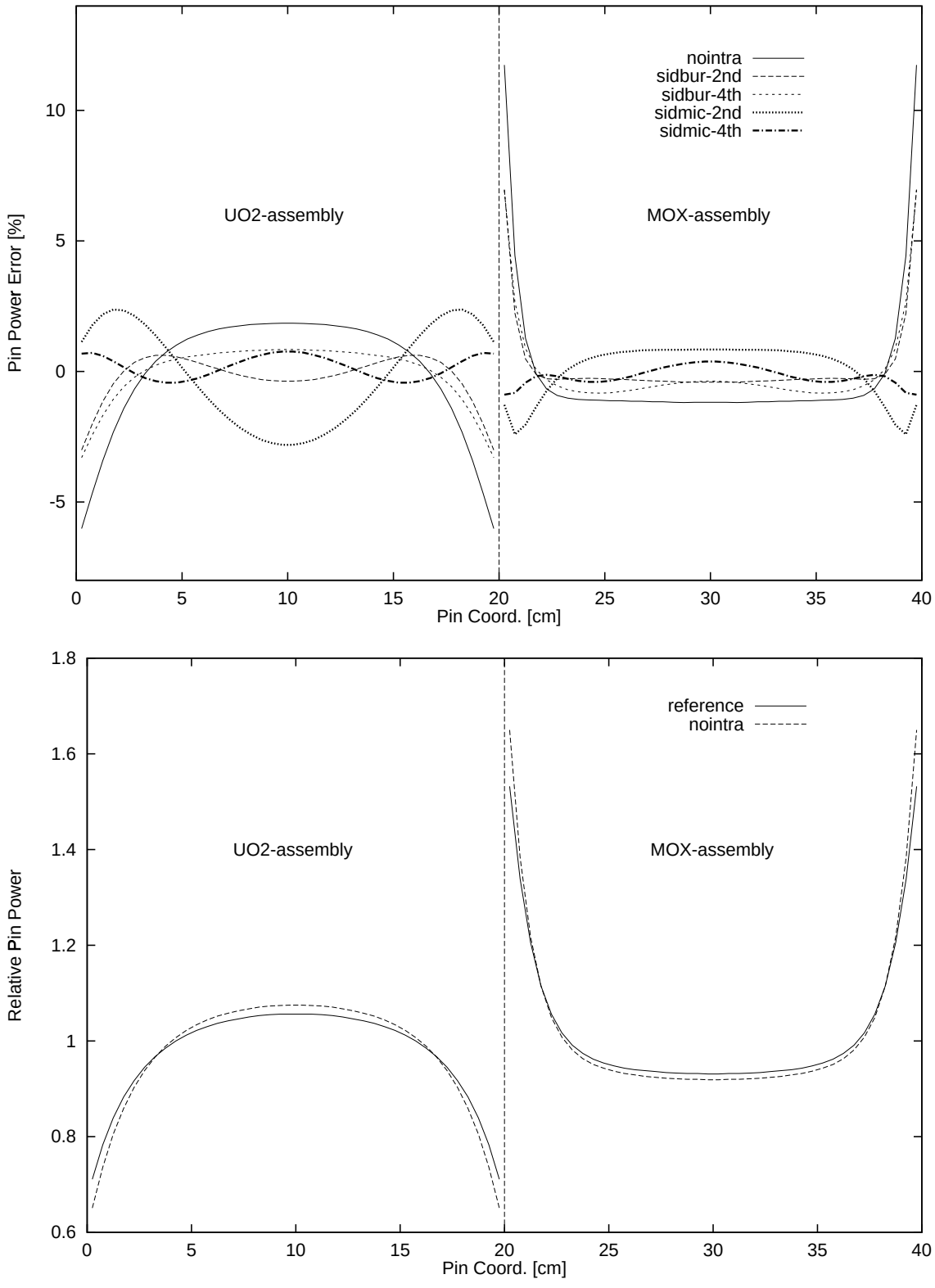

Figure 2. The relative pin powers and pin power errors for the MOX/UO_2 benchmark at 10 MWd/kg.

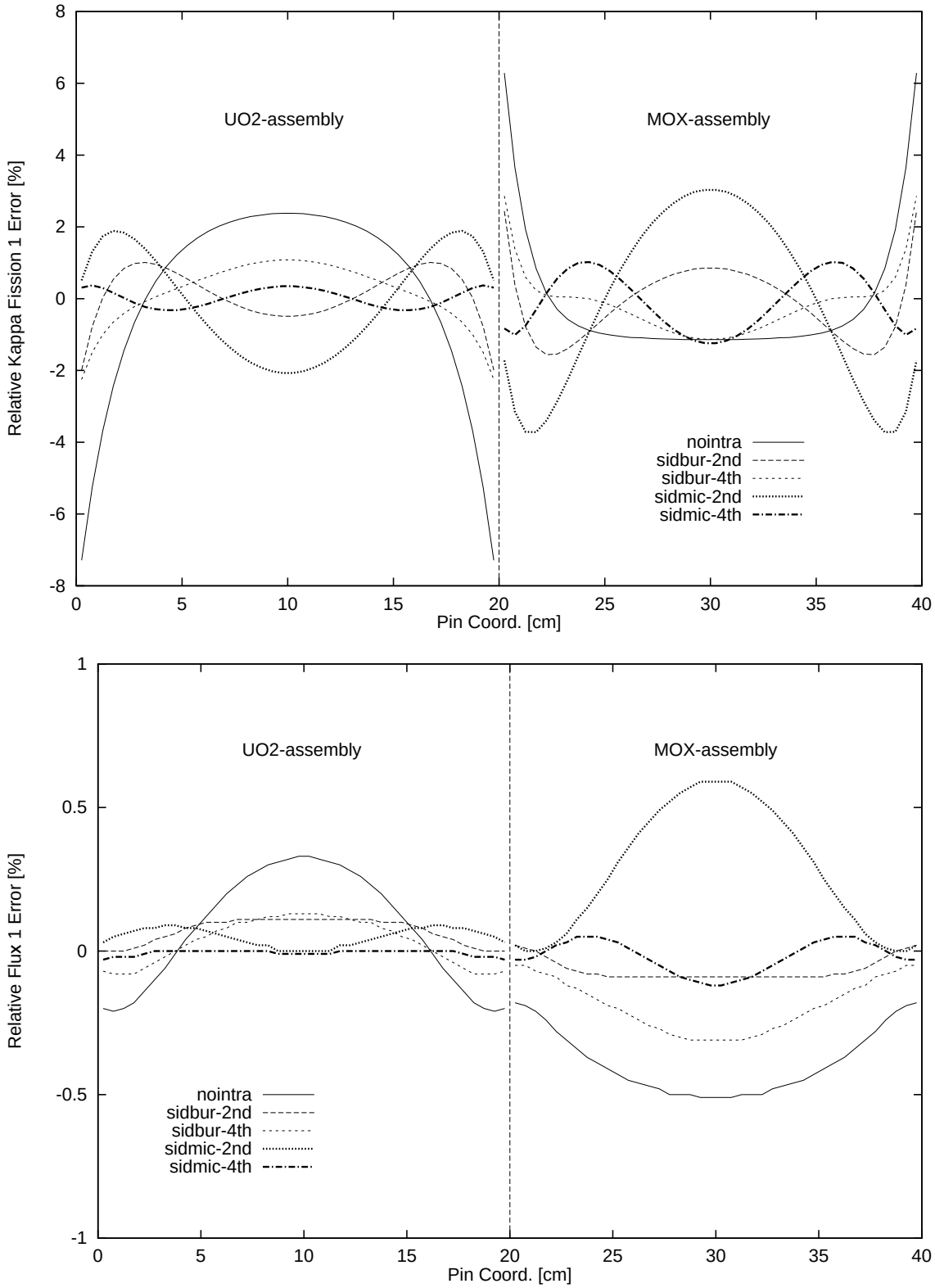

Figure 3. The relative errors in pin-integrated epithermal kappa-fission cross sections and epithermal fluxes for the MOX/UO_2 benchmark at 10 MWd/kg.

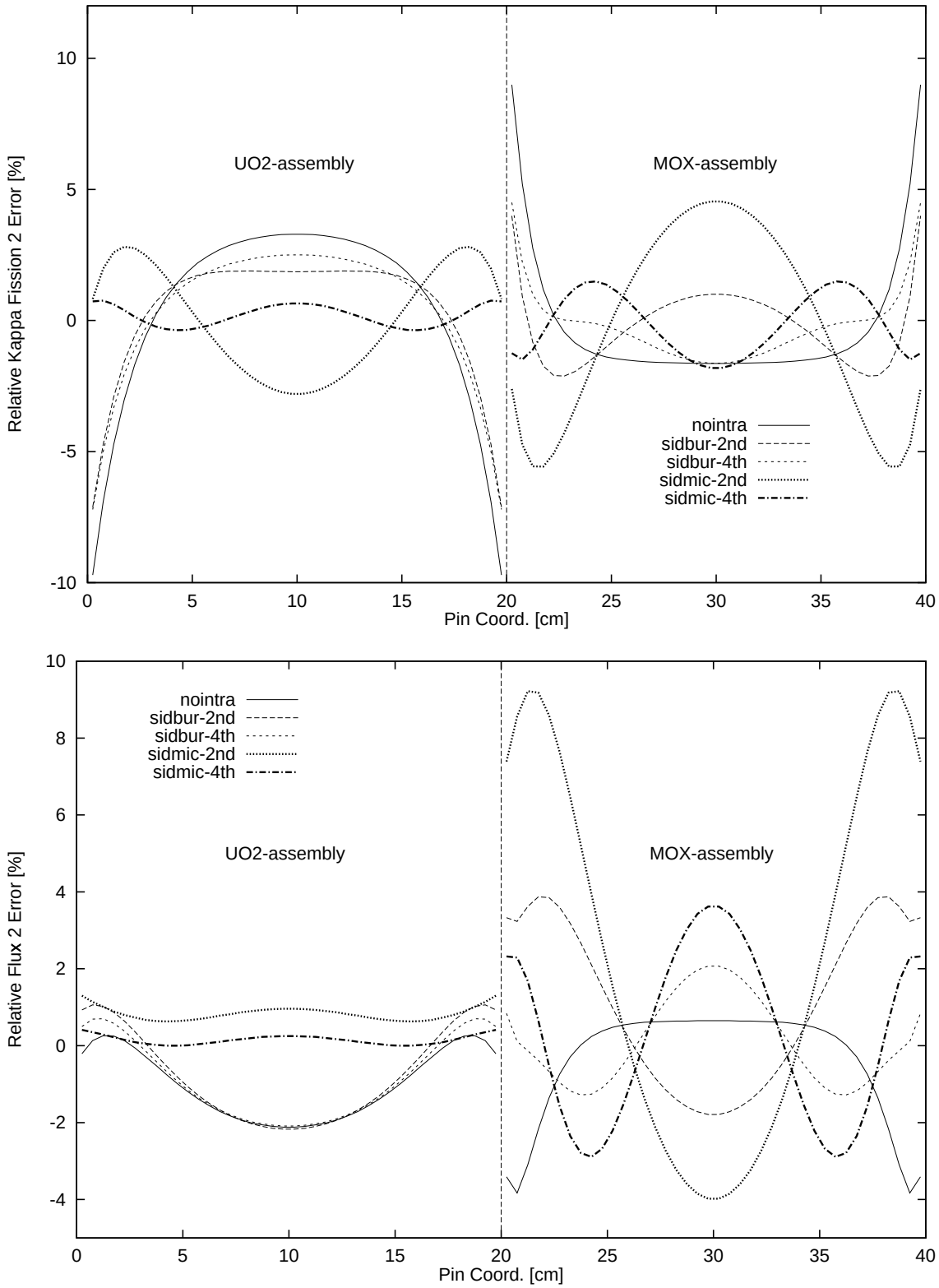

Figure 4. The relative errors in pin-integrated thermal kappa-fission cross sections and thermal fluxes for the MOX/UO_2 benchmark at 10 MWd/kg.

In addition to pin powers, accurate pin exposure values are usually also required (e.g., in thermal margin calculations). The correct method for obtaining such pin exposures is by time-integration of reconstructed pin powers over relevant irradiation periods. In practice, however, the pin exposures are usually computed by a similar reconstruction technique as used for the pin powers where a homogeneous intranodal exposure distribution is modulated with a single-assembly exposure form function. In the following, the accuracy of such a simplified approach is investigated. The homogeneous nature of the selected MOX/UO_2 test problem allows a clean analysis of the homogeneous component of this pin exposure reconstruction technique.

In figure 5 the pin-integrated exposures and their relative errors are shown. It is seen that an oscillating behaviour in the exposure errors is obtained which again indicates that a low order polynomial expansion fails to model the exponential character of the exposure distribution near material boundaries. Large relative errors (up to 30 % in the MOX assembly) are obtained with a second order polynomial expansion. The fourth order methods reduce the errors significantly although the remaining relative errors are still considered too large (10 %) to be acceptable.

It is observed that reconstructed pin exposures using the above technique have much larger errors than reconstructed pin powers using consistent orders of approximation. Since the accuracy requirements for pin exposure are similar to those for pin powers it is concluded that this technique is not acceptable especially if polynomials are used for representing the intranodal exposure spatial dependence. It is also suggested that reconstructed pin powers should directly be used for pin exposure determination.

5 CONCLUSIONS

In this paper depletion-history-induced intranodal effects on global (i.e., k_{eff} and nodal powers) and local (i.e., pin powers) parameters have been investigated. A simple, one-dimensional diffusion theory problem representing a PWR MOX/UO_2 core was used for this purpose.

It was demonstrated that it is important to account for intranodal effects in order to obtain accurate pin power predictions. The global parameters, on the other hand, were found to be less sensitive to such effects. Furthermore, it was observed that the combined use of intranodal isotopic inventory and exposure distributions for estimating the intranodal cross section behaviour significantly improves the accuracy in pin powers over the more traditional approach of utilizing exposure distributions only. A fourth order polynomial representation for the intranodal cross section distribution yields a pin power prediction accuracy of the order of 1 % and with a second order spatial representation pin power errors of the order of 3 % are obtained. However, it is important to bear in mind that reasonable results are obtained with low order polynomials due to a fortuituous cancellation of errors in the intranodal cross section and flux distributions, each of which shows a more or less oscillating spatial behaviour. This is an indication that a low order polynomial expansion fails to capture the pronounced exponential characteristics of the cross sections near the node boundaries, which suggests the use of exponential basis functions in combination with polynomials for obtaining an accurate intranodal cross section representation.

The importance of utilizing isotopic inventory data at node sides to determine side average macroscopic cross sections have been recognized by others,[9] although in practice the use of semi-explicit estimations of heavy nuclide number densities on node surfaces have been suggested. However, with the currently available computational capability, the explicit nuclide depletion on node sides is to be preferred over these more simplified approaches. On the other hand, explicit tracking of isotopics inside nodes, as performed in this work, is not considered practical due to the large number of spatial depletion points (especially in three

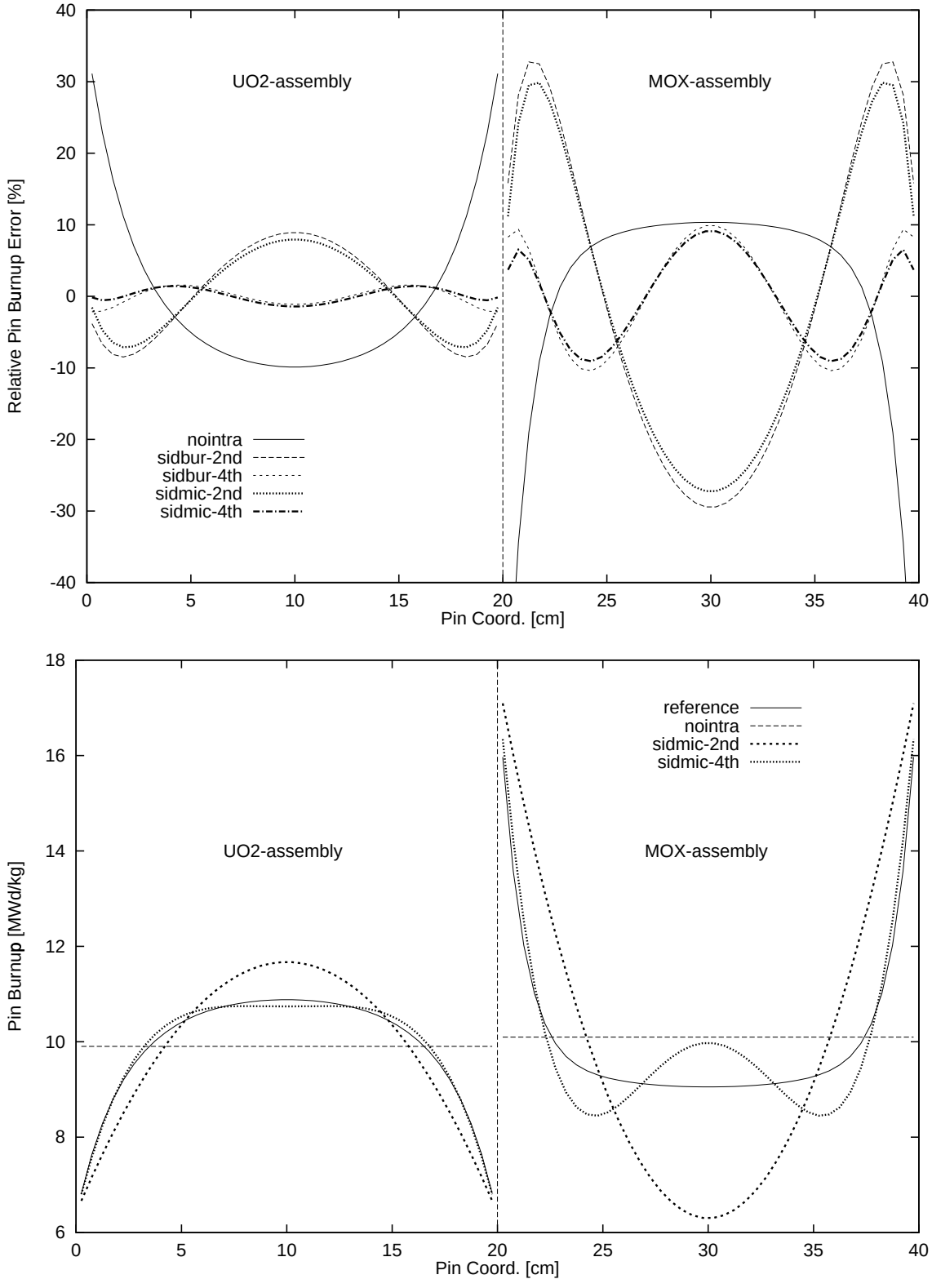

Figure 5. The pin exposures and relative pin exposure errors for the MOX/UO_2 benchmark at 10 MWd/kg.

dimensions) that may need to be used in order to obtain adequate spatial representation. In this regard, more elegant approaches for obtaining such intranodal nuclide inventory distributions have been proposed.[22,23]

Intranodal cross section models that take advantage of isotopic information are particularly attractive due to their generality in tracking nearly any kind of history phenomenon. Such models avoid many of the complications associated with traditional empirical (ad-hoc) models which require extensive and costly lattice calculations. However, further investigations are required to place the observations made in this work on a firmer basis, especially with regard to full three-dimensional reactor applications In addition, the question of suitable techniques for pin exposure reconstruction must be addressed if the same level of accuracy as for pin powers are to be attained.

ACKNOWLEDGEMENTS

This work was supported by the Center of Nuclear Technology, Stockholm, Sweden.

REFERENCES

1. R. D. Lawrence, "Progress in Nodal Methods for the Solution of the Neutron Diffusion and Transport Equations," *Prog. Nucl. Energy,* Vol. 17, No. 3, p. 271 (1986).

2. K. Koebke, "A New Approach to Homogenization and Group Condensation," IAEA-TECDOC 231, p. 303, International Atomic Energy Agency (Nov. 1978).

3. K. Koebke, "Advances in Homogenization and Dehomogenization," *Proc. Int. Topl. Mtg. Advances in Mathematical Methods for the Solution of Nuclear Engineering Problems,* Munich, FRG, April 27–29, 1981, Vol. 2, p. 59, Kernforschungszentrum Karlsruhe (1981).

4. K. S. Smith, "Assembly Homogenization Techniques for Light Water Reactor Analysis," *Prog. Nucl. Energy,* Vol. 17, No. 3, p. 303 (1986).

5. M. Lindberg, O. Norinder, "A New Homogenized Cell Data Structure for Use in a 3D Core Simulator," Jahrestagung Kerntechnik '90, p. 11 (1990).

6. S-Ö. Lindahl, E. Z. Müller, "Status of ABB Atom's Core Simulator POLCA," *Proc. Int. Conf. Physics of Reactors,* Mito, Japan (1996).

7. G. H. Hobson, R. C. Aigle, "Nodal Code Developments at Framatome/BWFC," *Topical Meeting on Advances in Reactor Physics,* Knoxville, April 1994.

8. R. Grummer, C. Lewis, S. Merk, "The SAV95 Code System for for PWR Core Design," *Proc. Am. Nucl. Soc. Topl. Mtg. Advances in Nuclear Fuel Management II,* Myrtle Beach, South Carolina, March 23–26, 1997, Vol. 1, p. 5-17.

9. H. Moon, "Advanced Core Design Using MICROBURN-B2 BWR Core Simulator," *Proc. Am. Nucl. Soc. Topl. Mtg. Advances in Nuclear Fuel Management II,* Myrtle Beach, South Carolina, March 23–26, 1997, Vol. 1, p. 5-47.

10. T. Ida, L. T. Mayhue, "Pu^{241}-Am^{241} Reactivity Effect Model in ALPHA / PHOENIX-P / ANC," *Proc. Int. Conf. Physics of Reactors,* Mito, Japan (1996).

11. T. Iwamoto, M. Yamamoto, "Development of a Multigroup Nodal BWR Core Simulator, NEREUS," *Proc. Int. Conf. Physics of Nucl. Sci. and Tech.,* Vol. 2, p. 1106, Long Island, New York (Oct. 1998).

12. M. R. Wagner, K. Koebke, H.-J. Winter, "A Nonlinear Extension of the Nodal Expansion Method," *Proc. Int. Topl. Mtg. Advances in Mathematical Methods for the Solution of Nuclear Engineering Problems,* Munich, FRG, April 27–29, 1981, Vol. 2, p. 43, Kernforschungszentrum Karlsruhe (1981).

13. S. Palmtag, K. S. Smith, "Two-Group Spectral Corrections for MOX Calculations," *Proc. Int. Conf. Physics of Nucl. Sci. and Tech.,* Vol. 1, p. 3, Long Island, New York (Oct. 1998).

14. M. Mori, M. Kawamura, "CASMO-4/SIMULATE-3 Benchmarking Against High Plutonium Content Pressurized Water Reactor Mixed-Oxide Fuel Critical Experiment," *Nucl. Sci. Eng.*, **121,** 41–51 (1995).

15. Y. A. Chao, Y. A. Shatilla, T. Ida, Y. Tahara "Challenges to Nodal Diffusion Methods for Cores with Mixed Oxide Fuel," *Proc. Int. Conf. Physics of Nucl. Sci. and Tech.,* Vol. 1, p. 9, Long Island, New York (Oct. 1998).

16. K. S. Smith, "Practical and Efficient Iterative Method for LWR Fuel Assembly Homogenization," *Trans. Am. Nucl. Soc.,* **71,** 238 (1994).

17. F. Rahnema, E. M. Nichita, "Leakage Corrected Spatial (Assembly) Homogenization Technique," *Ann. Nucl. Energy,* Vol. **24,** No. 6, pp. 477–488 (1997).

18. J. W. Malo, D. B. Lancaster, "Accounting for Deficiencies in the Diffusion Coefficient and Flux Approximation in Nodal Diffusion Theory," *Topical Meeting on Advances in Reactor Physics,* Knoxville, April 1994.

19. K. S. Smith, "An Analytical Nodal Method for Solving the Two-Group, Multi-Dimensional, Static and Transient Neutron Diffusion Equations," M.Sc. thesis, Massachusetts Institute of Techonology (1979).

20. D. L. Vogel, Z. J. Weiss, "A General, Multigroup Formulation of the Analytic Nodal Method," *Proc. Topl. Mtg. Advances in Reactor Physics,* Charleston, South Carolina, (1992).

21. C. H. Lee, Y. J. Kim, J. W. Song, C. O. Park, "Incorporation of a New Spectral History Correction Method into Local Power Reconstruction for Nodal Methods," *Nucl Sci. Eng.*, **124,** 160–166 (1996).

22. W. S. Yang, "A perturbation method for pointwise nuclide depletion calculations," *Ann. Nucl. Energy,* **26,** 265–275 (1999).

23. H. L. Rajic, A. M. Ougouag, "A Consistent Intranodal Burnup Correction Method for Advanced Nodal Depletion Analyses," *Proc. Int. Reactor Physics Conference,* Jackson Hole, Wyoming, Vol. III, p. 67 (1988).